International Journal of Engineering Research and Science & Technology

ISSN 2319-5991 www.ijerst.com
Vol. 4, Issuse.4,Oct 2016

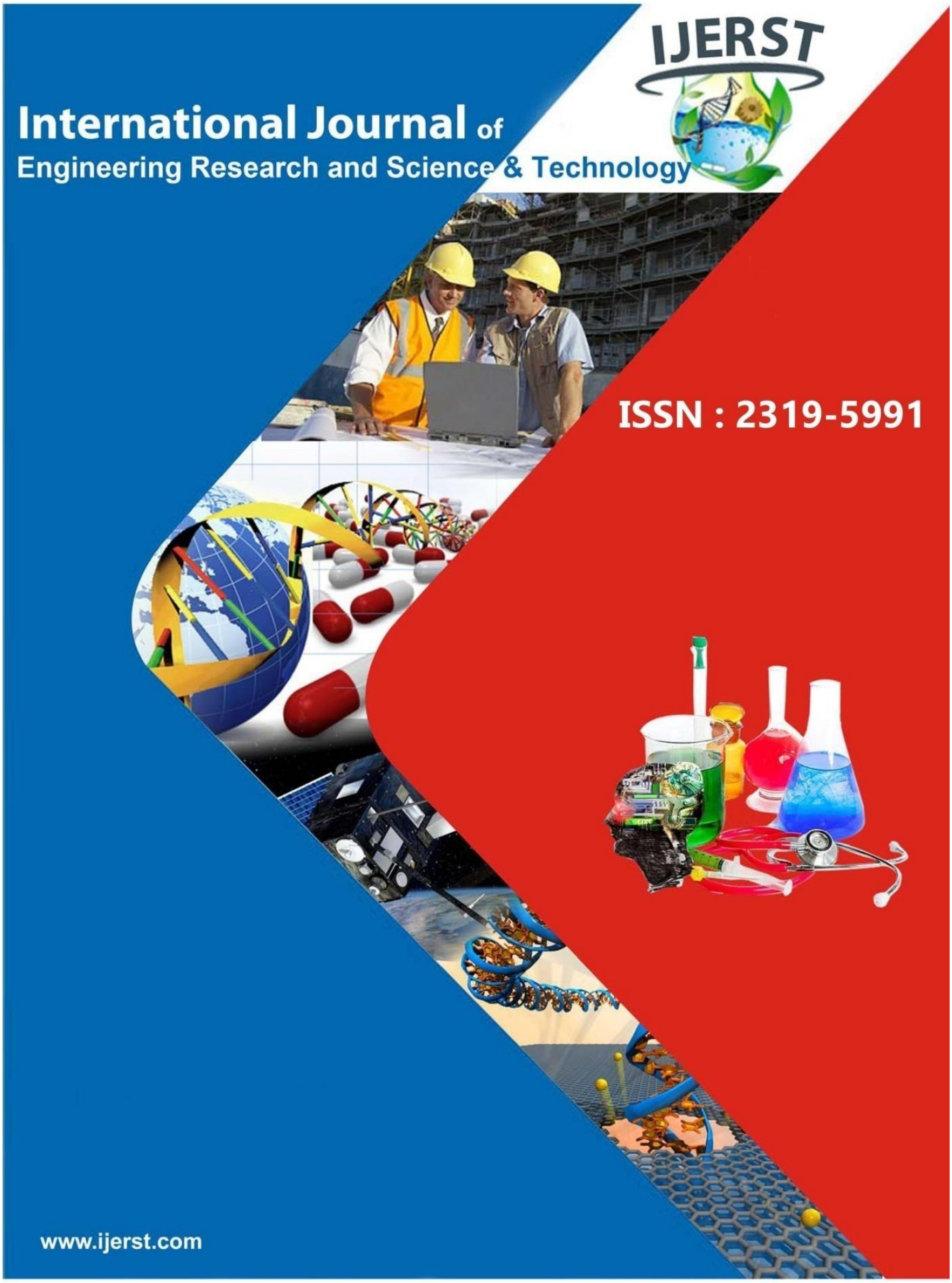

Email: editor@ijerst.com or editor.ijerst@gmail.com

International Journal of Engineering Research and Science & Technology
ISSN 2319-5991 www.ijerst.com
Vol. 4, Issuse.4,Oct 2016

Using the Recursive Method in OCTAVE and FEMM

Emmanuel by Tom Thampy Rajath Chandrashekar *, Raj Rivington

Additive and Smart Manufacturing Processes, Central Manufacturing Technology Institute, Bangalore, 560022, India
*Corresponding author: Emmanuel Gospel Raj Rivington,

ABSTRACT:

When a precise amount of flow or pressure regulation is needed, a proportional solenoid valve is the tool of choice. Designing the valve component, solenoid core, and coil for precise input and output ratings is necessary for manufacturing such valves. Magnetic qualities, application specific criteria like medical grade, temperature compatibility, etc. must all be taken into account when deciding on the materials for each part of the solenoid valve. To achieve proportional control, a linear relationship between the control input and the output of the proportional solenoid valve is essential. Achieving these goals relies heavily on optimizing the magnetic core. In order to achieve the required linearity in the plunger movement without sacrificing the actuation force on the plunger for a given size of the solenoid, it is essential to optimize the core geometry of the proportional solenoid. Based on performance criteria such as flow rate, pressure, and control needs such as the solenoid voltage and current ratings, a proportional solenoid valve is created for mass flow control in low pressure applications like medical oxygen ventilators. Valve components, such as medical-grade stainless steel with the necessary magnetic characteristics, are made from materials chosen on the basis of application needs. The optimal core shape of a proportional solenoid valve is calculated using a recursive method-based optimization methodology. In this paper, we show that the calculated values of plunger displacements from different offsets of 0 mm, 1 mm, and 2 mm from the reference position in a total stroke length of 5 mm closely match the experimental results obtained from the proportional solenoid valve manufactured based on optimization results.

KEYWORDS: Pressure regulator, Using a solenoid that is proportional to its size, Optimization via Recursion,

1. Introduction

The output flow or pressure of a proportional solenoid valve varies linearly with the input current or voltage. They find widespread usage in flow control settings that need accurate regulation of a metered flow of gas or liquid. Latching solenoids and proportional solenoids have distinct underlying geometries. Control input to the solenoid coil determines whether a latching solenoid valve is completely open or fully closed. Therefore, they function in two modes: full flow and no flow. On the other hand, proportional solenoids are preferred over latching types when a continuous range of motion is required for the plunger. To provide linear variation in valve output in terms of output flow or pressure, a well-designed proportional solenoid creates a linear displacement of the plunger. the output pressure that was achieved. Accuracy in the performance of proportional solenoids for automated valve control applications is determined primarily by the effective volume of the proportional solenoid, as well as the material and geometry of the solenoid core

Emmanuel by Tom Thampy Rajath Chandrashekar *, Raj Rivington

Additive and Smart Manufacturing Processes, Central Manufacturing Technology Institute, Bangalore, 560022, India
*Corresponding author: Emmanuel Gospel Raj Rivington,

2]. Because of the difficulty in designing a linear proportional solenoid valve, many scholars have proposed complex methods to improve the design of the solenoid and its use in valves [1, 3]–[8]. The basic geometries of an ON/OFF (or) latching solenoid are well-suited to the use of the standard force formulae [3, 9] available for computing the force on plunger for solenoids. It is impossible to use these equations [4, 9] to study the geometry of a proportional solenoid. This article details the creation of a direct-acting proportional solenoid valve for use in gas flow control and analyzes the factors that went into its design.

several variables, including magnet material, core shape, spring choice, valve geometry, and control. Its practical, recursive approach to solenoid optimization makes it a helpful summary of our knowledge of proportional solenoid design, development, and optimization. The combined power of the FEMM and OCTAVE software is used to visually depict the impact of different magnetic core diameters and the iterative optimization of the core shape. The effectiveness of the proportional solenoid is evaluated using FEM-based analysis to determine the best possible shape. In order to verify the findings, a working model of the proportional solenoid valve is built and tested.

2. The Proportional Flow Control Valve's Fundamental Parts

The co valve are shown

Design vindings,

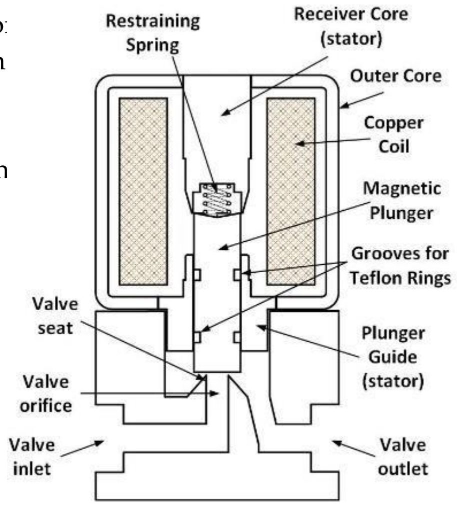

Figure 1 Cross section view of the proportional solenoid valve

A proportional valve consists of a solenoid, a magnetic core that acts as a low-reluctance path for the magnetic field, a magnetic plunger that moves when the solenoid is excited, a valve body with a valve closure mechanism that is actuated by the solenoid, and a spring that helps to keep the valve closed when the solenoid is unexcited. The stator core is hollow and houses a cylindrical plunger that travels in the direction of the stator receiver core, which is tapered.

core materials, and optimizing the core's proportional shape; designing a valve requires thinking about an orifice and a seat.

2.1 Winding Configuration

The flux produced by the winding of the proportional solenoid is sufficient to generate force, which in turn displaces the plunger and opens the valve. In contrast to an ON/OFF solenoid, a proportional solenoid does not latch during operation, hence it is crucial that the attractive force between the plunger and the stator be adequate and controlled over the whole range of the solenoid's stroke.

P = I2R (or VI (watt) (1) is the formula used to determine the amount of power used by the solenoid.

where,

I – Solenoid Current (A)

R – Resistance of the solenoid (Ω)

V – Voltage across the solenoid (V)

Force produced by the solenoid on the plunger[1], [9]

$$F = \frac{{(NI)_g}^2 \mu_0 A_g}{2g^2} \qquad (2)$$

where,

$(NI)_g$ – Ampere turns required (A)

μ_0 – Magnetic permeability of free space or vacuum (H/m) or (N/A²)

A_g – Area of the plunger surface (m2)

g – Length of the air gap (m)

$$8 = \frac{{(NI)_g}^2 4\pi \, x10^{-7} x \, \pi \, x \, (5.5 \, x10^{-3})^2}{2 \, x(1 \, x10^{-3})^2}$$

$$(NI)_g = \sqrt{\frac{8 \, x \, 2 \, x \, (1 \, x10^{-3})^2}{4\pi \, x \, 10^{-7} \, x \, \pi \, x \, (5.5 \, x10^{-3})^2}}$$

$$(NI)_g = 366 \text{ ampere turns(AT)}$$

Magnetic field intensity across the air gap cross section along the axial axis at the inner end [1, 2, 4]. Two Teflon rings [1] are used to decrease friction between the metal plunger and the plunger guide, and two circumferential grooves are provided on the plunger at appropriate positions to accept the rings.

Magnetic Flux density in the air gap,

$$B_g = \mu_0 \text{ x } H_g \quad (4)$$

$$= 4\pi \text{ x}10^{-7}\text{x } 366\text{x}10^{3}$$

$$B_g = 0.46 \text{ tesla(or) weber/sq. meter}$$

Total flux in the air gap,

$$\varphi_g = B_g \text{ x } A_g \quad (5)$$

$$= 0.46 \text{ x } \pi \text{ x } (5.5\text{x}10^{-3})^2$$

$$= 0.46 \text{ x } \pi \text{ x } (5.5\text{x}10^{-3})^2$$

$$\varphi_g = 43.7 \text{ weber}$$

To produce the same flux throughout a magnetic coreof same area Ag and a length of 200 mm:

Ignoring the fringing effect, the flux density in thecore, $B_c = B_g = 0.46$ tesla

Magnetic field intensity across the core

N = 2745 turns*Geometry of the Magnetic Core*

For a constant current, a proportional solenoid must deliver a constant force over its whole stroke length. This is made possible thanks in large part by the solenoid's central core and plunger's shape. In order for the solenoid to demonstrate linearity and repeatability

$$H_c = \frac{B_c}{\mu_c} \quad (6)$$

$$= \frac{0.46}{1000\text{x}4\pi\text{x}10^{-7}}$$

$$H_c = 366.1\text{A/m}$$

MMF required

$$(NI)_c = H_c\text{x length} \quad (7)$$

$$= 366.1\text{x } 200\text{x}10^{-3}$$

$$(NI)_c = 73.2 \text{ AT}$$

Total Ampere turns required:

$$(NI)_{total} = (NI)_c + (NI)_g \quad (8)$$

$$= 73.2 + 366$$

require number of turns

$$N = \frac{549}{0.2} \quad (9)$$

of the control motions of the plunger, it is necessary to adjust the control parameters D, t, and P, as shown in Figure 2 [2]. P is the depth of the conical top of the plunger, D is the corner point on the outside border of the cone, and t is the corner point on the top of the cone.

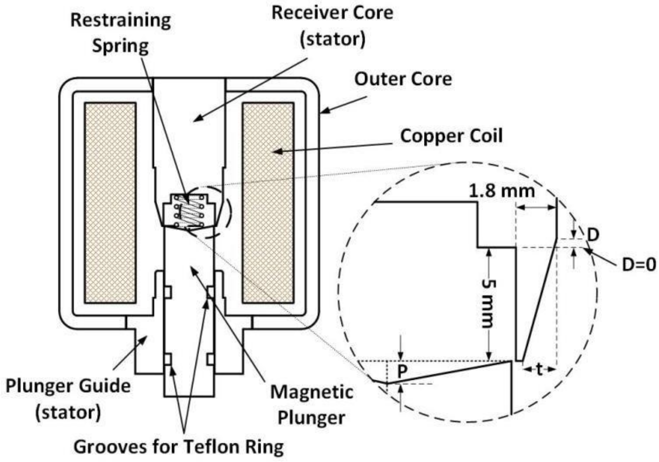

Figure 2 Cross section of the proportional solenoid depicting the conedesign parameters

The typical Force-Displacement characteristic of a As may be seen in Figure 3 (a), a proportionate solenoid. In a perfect world, the solenoid's force for a given current for plunger displacement is constant over the whole stroke length [3, 6]. The current via the solenoid increases this force. A linear force, with a slope proportional to the spring constant, is generated by the restraining spring sandwiched between the plunger and the receiver core. The

(NI)total

= 439.2 AT

points where the solenoid's force meets the spring's force Plunger equilibrium points are shown by curves.

Adding an extra 25% to account for losses,

Total (NI) = 549 A.T.
Having a 0.2 A (or 200 mA) control current would shifts for varying solenoid current levels [2, 6]. Figure 3 (b) displays the resulting connection between solenoid current and plunger displacement.

The Control Cone Is Optimised Recursively
Adjusting the settings on the cone of control (D,

linear properties of the plunger movement relative to the control input from the solenoid, t, and P are crucial. Comparative study of force calculation methods for the
where,

∑ X=1(F(n) − Favg)

f(s) =

x

Finite Element Method Magnetics (FEMM) software is used for the plunger [2, 7, 10]. The specifics of the mesh's configuration are shown below.

Type of Mesh: Triangles

Adjustable Mesh Size

The optimization of the design parameters is made easy using the recursive technique, which takes just two rounds before yielding the best possible outcomes. The supplied solenoid is developed with the configuration shown in Fig. 2, optimized for the three independent variables of D, t, and P. However, construction of proportional solenoids with alternative configurations is conceivable with many parameters that can be optimized. The recursive procedure iteratively determines the best place for each parameter, starting with a broad search and becoming more specific with each step.

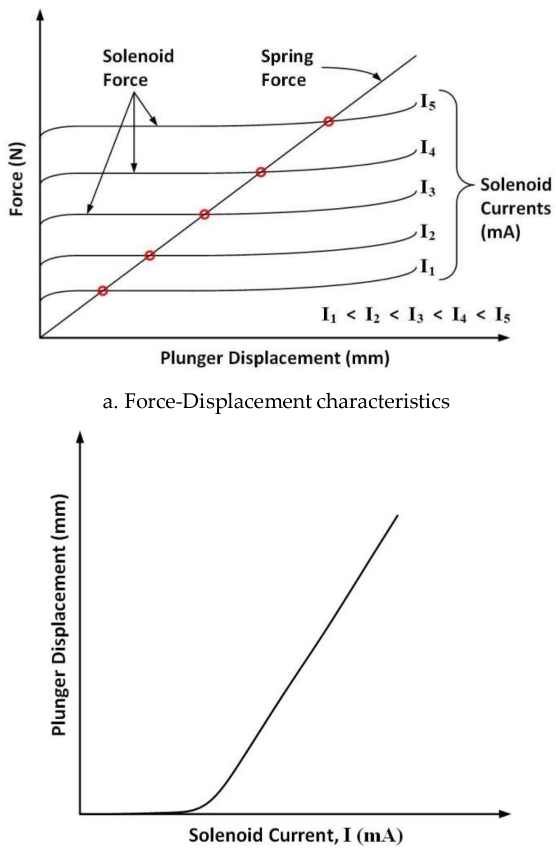

a. Force-Displacement characteristics

b. Displacement-Current characteristics

Figure 3 Typical characteristics of a proportional solenoid

The optimization of the cone parameters of the proportional solenoid is based on minimizing the objective function f(s) [2], [6], [10] shown below:
f(s) – Objective function (N)
x – Number of plunger steps
F(n) – Force on plunger on n^{th} step (N)
F_{avg} – Average force on plunger across the full stroke length (N)

3.1. First iteration
Each recursive algorithm iteration for optimizing the proportional solenoid shape involves a series of stages to determine the parameters' near-optimal values in the given order (D, t, and P). The Force vs. Displacement curves are obtained by moving the plunger from the tip of the cone to a distance of 4 mm,

with a step size of 0.5 mm, for each location of D between the limits of -5 mm and +5 mm, as illustrated in Figure 4. Figure 5 depicts the force versus displacement curves for a range of D values. Having D be the corner point at about -5 mm demonstrates a high force near the tip of the stationary core because of the large area made available by virtue of the position of D, and a decreasing force as the plunger moves deeper inside the core because of the increased area of low reluctance core appearing in the radial direction rather than the axial direction. As the receiver cone becomes acute and conical as point D rises, the force exerted on the plunger over its whole stroke becomes modest. Figure 6 shows that the objective function has its highest values when D is very far from the reference point, and its lowest value of roughly 0.6 when D is very little more than 1 mm above the reference position.

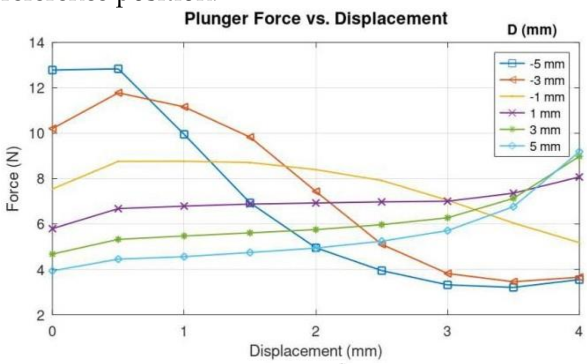

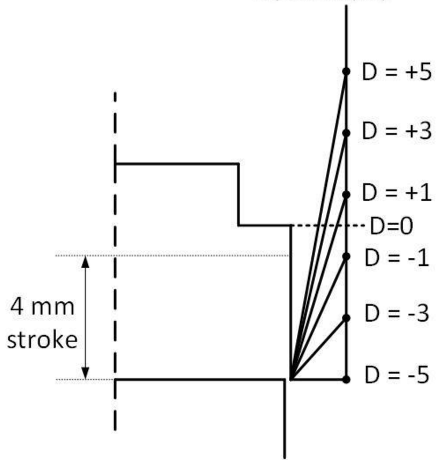

Figure 4 Optimization of D in the first iteration

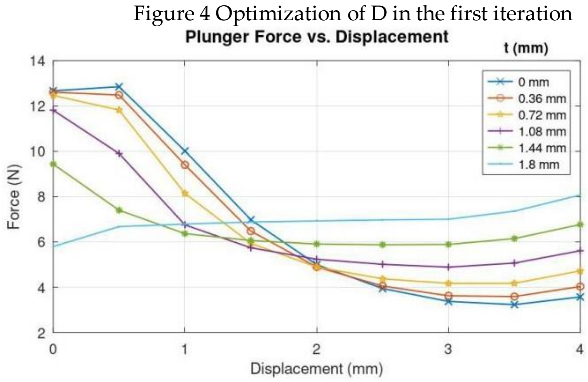

Figure 5 Plunger Force vs. Plunger Displacement characteristics for various positions of D in the first iteration

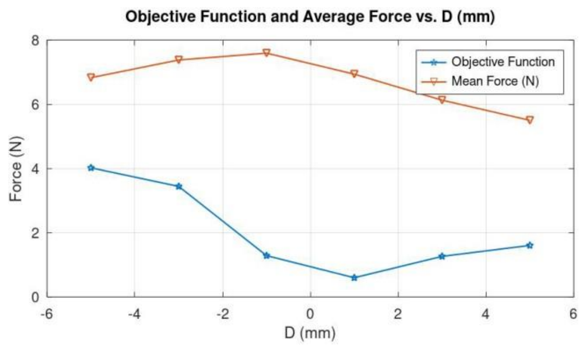

Figure 6 Objective function and Average force at various positions of D in the first iteration

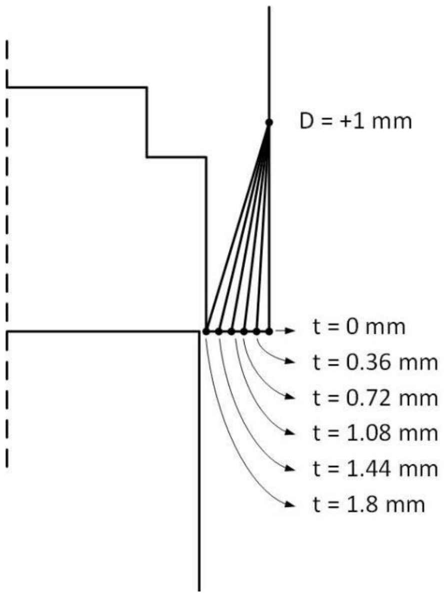

In the following recursive iteration, we'll optimize t within the constraints of 0 mm and 1.8 mm, fixing the optimum value of D at 1 mm acquired in the previous stage. As can be seen in Figure 7, when D is set to 1 mm, t is moved in increments of 0.36 mm, from 0 to 1.8. Figure 8 shows many plots of force against plunger displacement, and the one for t=1.8 seems flatter than the others. As can be seen in Figure 9, the Objective function is similarly at its lowest at a t value of 1.8 mm.

Figure 7 Optimization of t in the first iteration

Figure 8 Plunger Force vs. Plunger Displacement characteristics for various positions of t in the first iteration

The positions of D and t are fixed at 1 mm and 1.8 mm respectively from their references and the parameter P is next optimized.

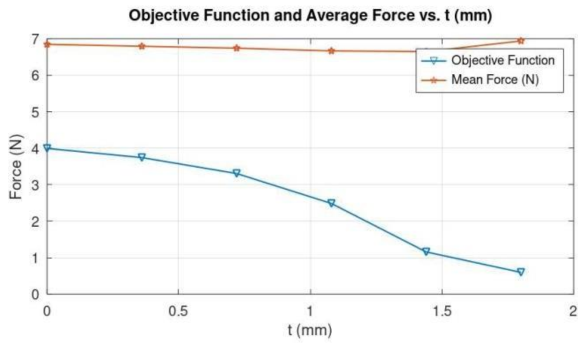

Figure 9 Objective function and Average force at various positions of t in the first iteration

Because P lies on the axis of the cylindrical plunger, shifting P inside the plunger's structure results in a hollow conical shape on the plunger's surface opposite the receiver core. P changes from -5 mm to 0 mm in 1 mm increments, as shown in Figure 10.

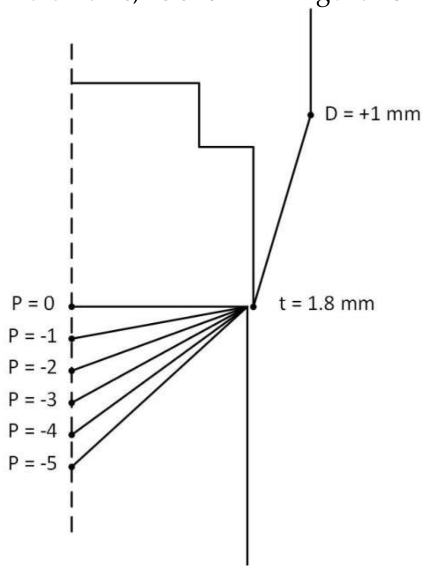

Figure 10 Optimization of P in the first iteration

The force characteristics for various positions of P can be seen in Figure 11 and the objective function characteristics in Figure 12. The optimization of P would

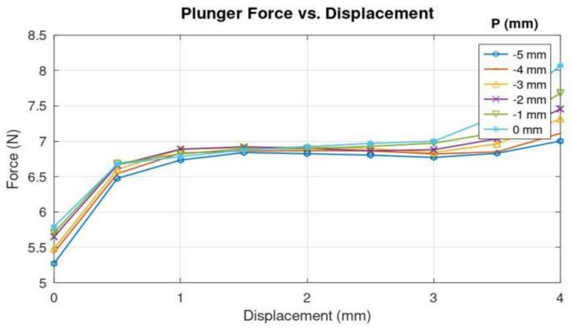

have a major effect on minimizing the plunger's latching propensity when it approaches the stationary receiver core beyond 3.5 mm.

Figure 11 Plunger Force vs. Plunger Displacement characteristics for various positions of P in the first iteration

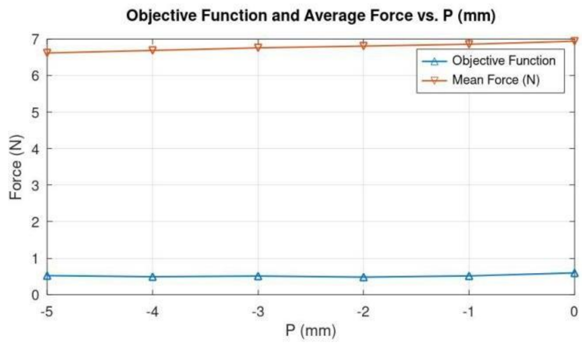

Figure 12 Objective function and Average force at various positions of P in the first iteration

TABLE 1 displays the summary of parameters, constraints, and optimization outcomes from the first iteration of the recursive approach. Figure 13 depicts the final result of the first iteration in terms of geometry.

Table 1: Optimization results obtained from the First Iteration of the recursive method

Parameter	Min	Max	Step size (mm)	Optimal	Min. F(s)	Average force at Min. F(s)
D	-5	5	2	1	0.59828	6.9384
t	0	1.8	0.36	1.8	0.59828	6.9384
P	-5	0	1	-2	0.48351	6.8065

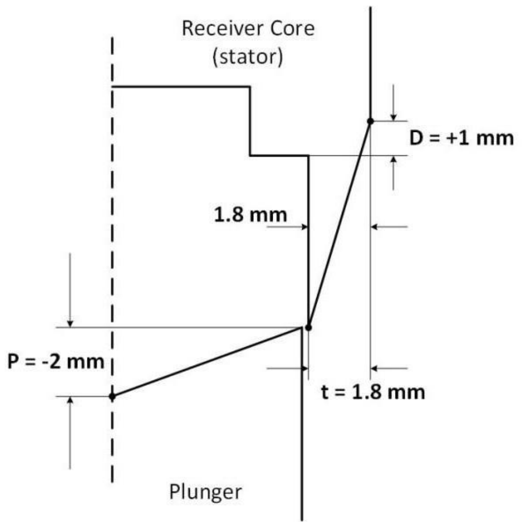

Figure 13 Geometry of proportional solenoid core obtained from First iteration of recursive optimization.

3.2. Second Iteration

The optimum positions of the geometrical parameters have been roughly estimated by the first iteration of the recursive technique. To get reliable results of the optimization parameters, a second iteration is often necessary. See TABLE 2 for a complete breakdown of the updated requirements, optimum values, and resulting objective function for the parameters. In order to do a thorough search for the precise positions of the parameters, fresh restrictions are introduced with small step sizes around the previously achieved best findings. From the first row of TABLE 1 to the final row of TABLE 2, the value of the Minimal Objective Function drops from around 0.59 to 0.15.

Table 2: Optimization results obtained from the Second Iteration of the recursive method

Paramete r	Mi n	Ma x	Step size (mm)	Optim al	Min. F(s)	Average force at Min. F(s)
D	0	2	0.4	0.4	0.40518	7.131
t	1.3	1.8	0.1	1.7	0.18655	6.9748
P	-3	-1	0.2	-1	0.14875	7.0161

The recursive optimization of D, t, and P yielded the force curves and objective function curves seen in Figures 14–19. Parameters P = +0.4 mm, t = +1.7 mm, and P = -1 mm are shown to be ideal. Figure displays the ideal proportional core shape of the solenoid. 20.

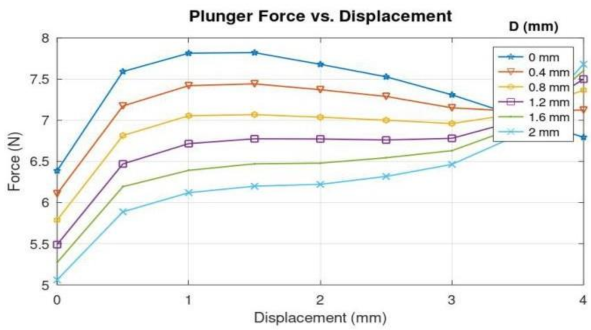

Figure 14 Plunger Force vs. Plunger Displacement characteristics for various positions of D in the second iteration

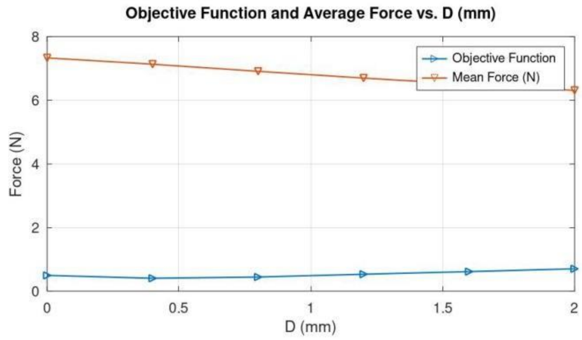

Figure 15 Objective function and Average force at various positions of D in the second iteration

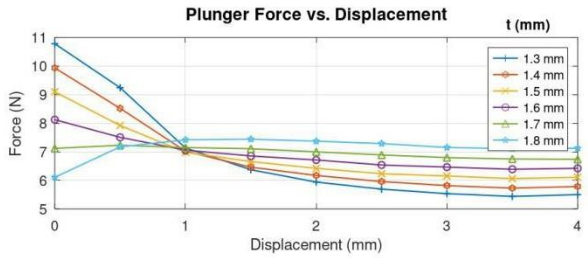

Figure 16 Plunger Force vs. Plunger Displacement characteristics for various positions of t in the second iteration

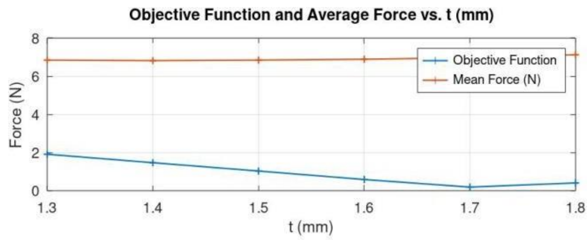

Figure 17 Objective function and Average force at various positions of t in the second iteration

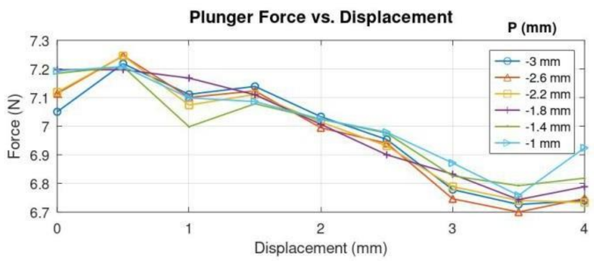

Figure 18 Plunger Force vs. Plunger Displacement characteristics for various positions of P in the second iteration

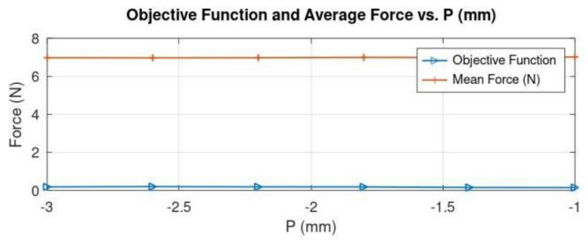

Figure 19 Objective function and Average force at various positions of P in the second iteration

Figure 21 shows the proportional solenoid valve that is developed with the optimized core geometry for gas flow at a maximum pressure of 3 Bar.

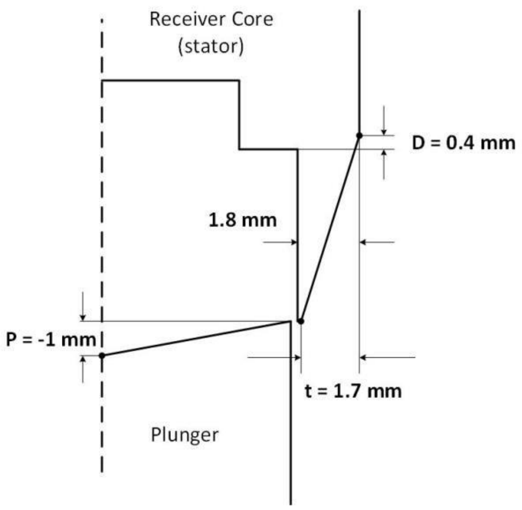

Figure 20 Geometry of the optimized proportional solenoid core obtained from second iteration of recursive method.

2. Performance testing and results

If you want top performance from your proportional solenoid, you need to make sure its shape is optimum. Constant force for constant current through the solenoid winding has been achieved by optimizing the proportional solenoid shape across the range of the 4 mm stroke length during which the solenoid is designed to function.

Figure 23 displays the load line and force curves of the optimized solenoid for different constant currents. The load line represents the force created by the restraining compression-spring with a spring constant of 3.6 N/mm.

Figure 21 The developed proportional solenoid valve for flow control

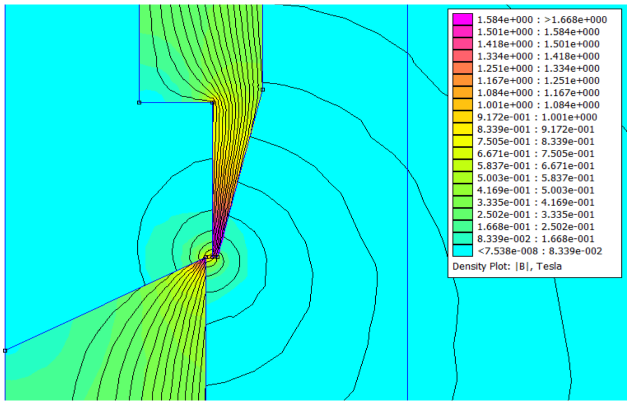

Figure 22 Magnetic flux density plot of the optimized proportional solenoid geometry in FEMM

The characteristics between solenoid current and the plunger displacement are shown by finding the points where the load line and the force curves overlap (Figure 24).

Figure 23 Force vs Displacement characteristics of the Proportional

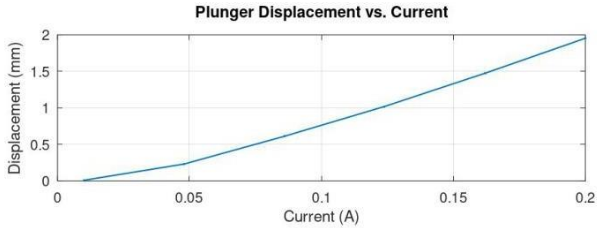

Figure 24 Plunger displacement vs solenoid current characteristics with 0 mm offset of the restraining spring

Regardless of the spring's starting offset or the plunger's beginning location, the relationship between the control current and the plunger displacement stays the same for a well-tuned proportional solenoid.

Figure 25 depicts the force curves of the proportional solenoid and the load line of the spring with a 1 mm offset. Plunger displacement and solenoid control current exhibit the characteristics shown in Figure 26. It's important to keep in mind that the offset position of the spring is only 1 mm to begin plunger displacement.

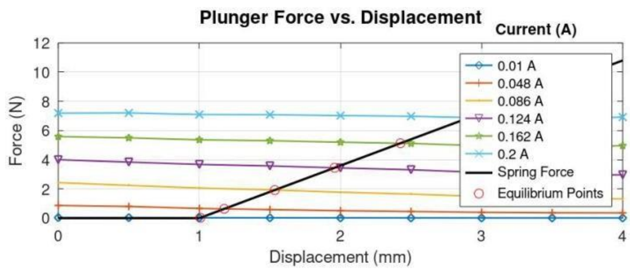

Figure 25 Force vs Displacement characteristics of the Proportional Solenoid and the restraining spring (1 mm offset)

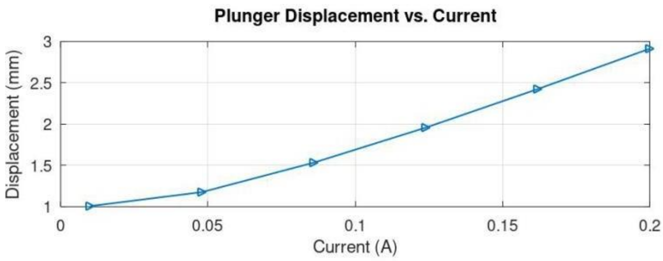

Figure 26 Plunger displacement vs solenoid current characteristics with 1 mm offset of the restraining spring

Figure 27 depicts the proportional solenoid force curves and the load line of the spring that is off by 2 mm. Figure 28 depicts the relationships between the solenoid control current and the plunger displacement. The 2 mm offset location of the spring is where the plunger's displacement really begins.

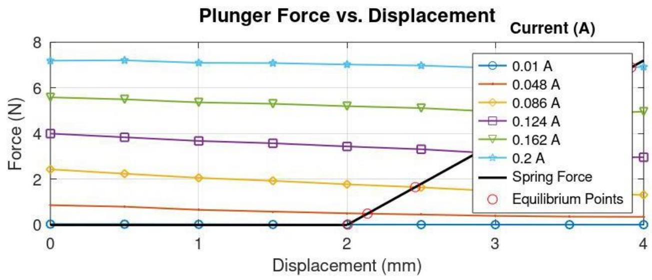

Figure 27 Force vs Displacement characteristics of the Proportional Solenoid and the restraining spring (2 mm offset)

Figure 29 depicts the effective plunger displacement in the

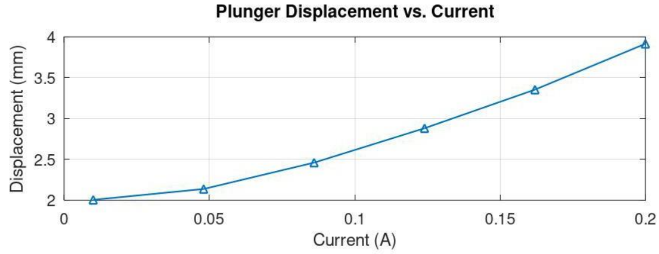

optimized model of the proportional solenoid with zero, one, and two millimeter offsets, respectively. It's clear that the traits are comparable to one another. It's important to keep in mind that perfect qualities include having perfectly straight and matched curves.

Figure 28 Plunger displacement vs solenoid current characteristics with 2 mm offset of the restraining spring

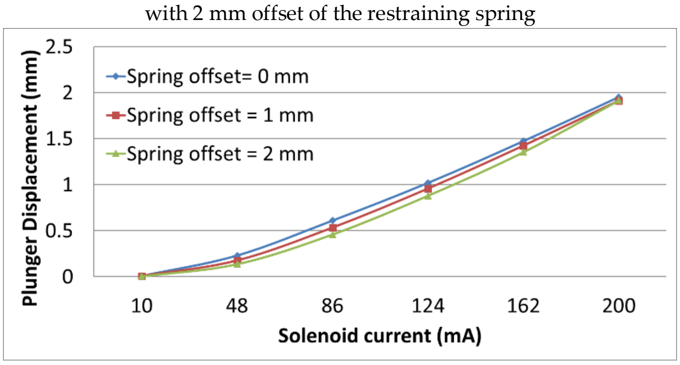

Figure 29 Effective plunger displacement vs solenoid current characteristics of the optimal design with various offsets

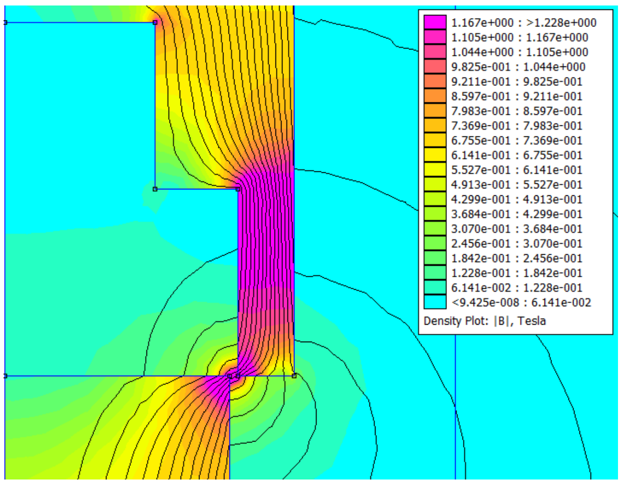

Figure 30 Magnetic flux density plot of the flat non-optimal geometryin FEMM

When the design isn't ideal, the control characteristics may not be as neat and tidy as you'd want. Figure 30 and Figure

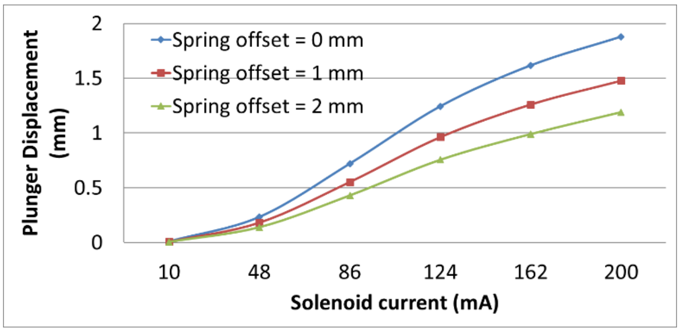

32 both depict non-optimal designs, one of which is flatter than the best form while the other is sharper.

Figure 31 Effective plunger displacement vs solenoid current characteristics of the flat non-optimal design with various offsets

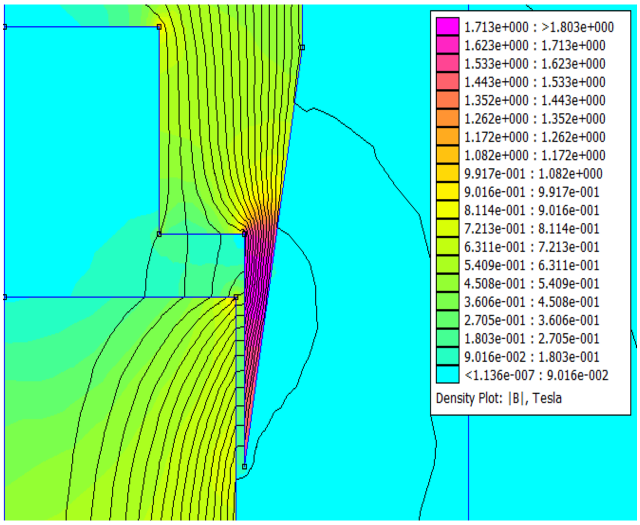

Figure 32 Magnetic flux density plot of the sharp non-optimalgeometry in FEMM

The characteristics of the two non-optimal designs are shown in Figure 31 and Figure 33. An undesirable widening in characteristics can be seen in Figure 31 corresponding to a flat non-optimal geometry. It can be seen in Figure 33 that two of the curves are close to each other with lesser displacement than optimal and the thirdcurve is deviating.

The Plunger displacement vs current characteristics is experimentally obtained from the manufactured proportional solenoid and compared with the computed characteristic of the optimized geometry as shown in Fig 34.

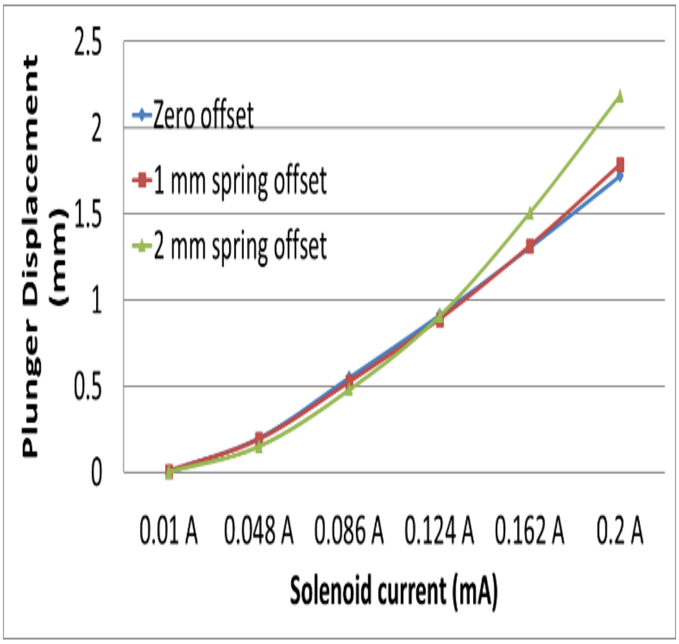

Figure 33 Effective plunger displacement vs solenoid current characteristics of the sharp non-optimal design with various offsets

Figure 34 compares the experimental displacements from initial offsets of 0 mm, 1 mm, and 2 mm with the corresponding computed displacements with the aim of achieving an optimized geometry of proportional solenoid to produce linear displacement for coil currents regardless of the initial offset.

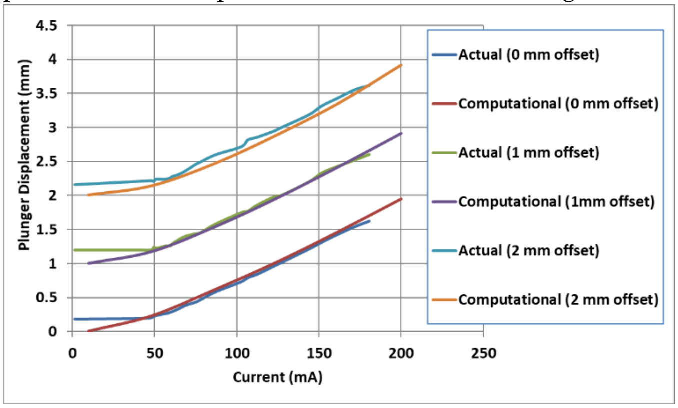

Figure 34 Experimental plunger displacement and computed plungerdisplacement

3. The graphs indicate good agreement between measured and calculated values, verifying the recursive methodology used in the suggested optimization strategy. Due to the plunger being towards the far end of the proportional cone, the actual displacement with 0 mm offset is slightly smaller than the computed displacement. Force on plunger tends to be larger and displacement greater as offset increases, i.e. when the plunger position is well within the proportional cone. When the plunger moves too far within the proportional cone, the displacement flattens because the air gap flux is now more laterally oriented than axially. This happens for increasingly large offsets.

Conclusion

The methodological framework for creating a proportional solenoid valve has been detailed in this study. We have covered the fundamentals of proportional solenoid functioning, as well as material choices and power supply-related design considerations. This paper focuses mostly on optimizing the proportional core, since this is one of the most important elements in developing a proportional solenoid. Due to its efficiency in generating optimization results in less than three rounds, the recursive technique of optimization is employed to determine the optimal shape of the proportional core of the solenoid valve. Diagrams and graphs show the step-by-step procedure for optimizing the geometrical parameters of the proportional core. The best-possible hardware implementation of the proportional solenoid valve is built and evaluated. The findings show that linear displacement for the solenoid current was seen throughout a range of offsets when the proposed approach of optimizing a proportional solenoid was used. This technical study details a method for designing proportional solenoid valves that may be used in a wide range of settings.

.

References

J Braz. Soc. Mech. Sci. Eng., vol. 43, no. 60, 2021, doi:10.1007/s40430-020-02768-7 cites "Multi-objective genetic algorithm optimization of linear proportional solenoid actuator" by S.J. Wang et al.

S.N. Yun et al. presented "New approach to design control cone for electro- magnetic proportional solenoid actuator" at the 2012 IEEE/ASME International Conference on Advanced Intelligent Mechatronics (AIM), which can be found online at https://doi.org/10.1109/AIM.2012.6265943.

Multiobjective Optimization of a Hollow Plunger Type Solenoid for High Speed On/Off Valve, S. Wu, et al., IEEE Transactions on Industrial Electronics, 65(4), 3115-3124, 2018, https://doi.org/10.1109/TIE.2017.2756578.

System Modeling, Coupling Analysis, and Experimental Validation of a Proportional Pressure Valve with Pulse Width Modulation Control, F. Meng et al., IEEE/ASME Transactions on Mechatronics, volume 21, issue 3, pages 1742-1753, 2016, https://doi.org/10.1109/TMECH.2015.2499270.

In 1988, IEEE's Transactions on Industry Applications published "Finite-element analysis of a constant-force solenoid for fluid flow control," written by P.B. Lequesne (https://doi.org/10.1109/28.6107).

In 2002, SAE published T. Arakawa's "Optimization Technology of Magnetic Circuit for Linear Solenoid" (https://doi.org/10.4271/2002-01-0565).

24th Telecommunications Forum (TELFOR), 2016, https://doi.org/10.1109/TELFOR.2016.7818839 Plavec, E., & Vidovic, M. "Genetic algorithm-based plunger shape optimization of DC solenoid electromagnetic actuator"

Shape optimization of solenoid actuator using the finite element approach and numerical optimization methodology. Sang-Baeck Yoon, JinHur, Yon-Do Chun, and Dong-Seok Hyun. IEEE Transactions on Magnetics. vol. 33, no. 5. pp. 4140-4142. 1997. https://doi.org/10.1109/intmag.1997.597697.

From the COMSOL Conference Proceedings, Stuttgart, 2011: Vogel, O., and Ulm, J., "Theory of Proportional Solenoids and Magnetic Force Calculation Using COMSOL Multiphysics."

[10] In 2005, Jae Seop Ryu, Yingying Yao, Chang Seop Koh, Sonam Yun, and Dong Soo Kim published "Optimal Shape Design of 3-D Nonlinear Electromagnetic Devices Using Parameterized Design Sensitivity Analysis" in IEEE Transactions on Magnetics, volume 41, issue 5.